PHYSICAL REVIEW E **84**, 050102(R) (2011)

Discontinuous percolation transitions in real physical systems

Y. S. Cho and B. Kahng
Department of Physics and Astronomy, Seoul National University, Seoul 151-747, Korea
(Received 21 March 2011; revised manuscript received 6 September 2011; published 23 November 2011)

We study discontinuous percolation transitions (PTs) in the diffusion-limited cluster aggregation model of the sol-gel transition as an example of real physical systems, in which the number of aggregation events is regarded as the number of bonds occupied in the system. When particles are Brownian, in which cluster velocity depends on cluster size as $v_s \sim s^{\eta}$ with $\eta = -0.5$, a larger cluster has less probability to collide with other clusters because of its smaller mobility. Thus, the cluster is effectively more suppressed in growth of its size. Then the giant cluster size increases drastically by merging those suppressed clusters near the percolation threshold, exhibiting a discontinuous PT. We also study the tricritical behavior by controlling the parameter η, and the tricritical point is determined by introducing an asymmetric Smoluchowski equation.

DOI: 10.1103/PhysRevE.84.050102 PACS number(s): 64.60.ah, 02.50.Ey, 89.75.Hc

Percolation, a stochastic model for the formation of macroscopic-scale spanning clusters, has received considerable attention in statistical physics for a long time as a model for metal-insulator transitions, sol-gel transitions, epidemic spreading, fracture, and so on [1,2]. When a control variable, which is the occupation probability of a conducting bond between two vertices, is increased, a long-range spanning cluster emerges at a critical threshold p_c. Such a percolation transition (PT) is conventionally continuous. The discovery of a *discontinuous* PT has therefore been a longstanding issue in statistical physics. In these circumstances, a recently introduced stochastic model [3] for the explosive PT has attracted considerable attention in a short time period. This stochastic model is a simple modification of the classical Erdős-Rényi (ER) random graph model [4], which contains a suppression effect in the growth of cluster sizes. Such an explosive PT behavior has also been observed in other recently introduced stochastic toy models [5–11]. Even though there is controversy with regard to whether such an explosive PT is indeed discontinuous in the thermodynamic limit [12–14], the explosive percolation model has opened an avenue for the study of discontinuous PTs in nonequilibrium systems. In this Rapid Communication, we examine in what physical systems in the real world discontinuous PTs can be observed.

In this Rapid Communication, we consider the diffusion-limited cluster aggregation (DLCA) model [15–17] for the sol-gel transition as a candidate for our purpose. This model was introduced a long time ago, and the dynamic cluster-size distribution was intensively studied for this model [18–22]. Here, this model is studied in the context of PT, which takes place as the number of cluster aggregation events increases. We also show that the DLCA model indeed exhibits a discontinuous PT. Furthermore, we generalized the DLCA model in which cluster velocity depends on cluster size as $v_s \sim s^{\eta}$. As the parameter η varies, there exists a tricritical point beyond which the PT becomes continuous with continuously varying exponents. We show that the generalized DLCA model can be represented via an asymmetric Smoluchowski equation, by which the tricritical point can be determined.

Even though real physical systems are in three dimensions, we perform simulations extensively in two dimension as follows: Initially, N single particles are placed randomly in $L \times L$ square lattices. Simulations start from N monoparticles. The density of the particles is given as $\rho = N/L^2$. The system size L is controllable, while the density remains fixed in the simulations. Here we consider the case in which the particles are Brownian, so that velocity of a cluster is inversely proportional to the square root of its size [23]. To implement, we perform simulations as follows [17]: At each time step, (i) an s-sized cluster is selected with the probability $q \equiv s^{-0.5}/(\sum_s N_s s^{-0.5})$, and is moved to the nearest neighbor. When two distinct clusters are placed at the nearest-neighbor positions, these clusters are regarded as being merged, forming a larger cluster. (ii) The time is advanced by $\delta t = 1/(\sum_s N_s s^{-0.5})$, where N_s is the number of s-sized clusters. We iterate steps (i) and (ii) until the giant cluster size is N. Later, we will consider a more general case in which the velocity is proportional to s^{η} [20]. Numerical simulations are also carried out in three dimensions, and the behavior of the PT in three dimensions is similar to that in two dimensions.

When we study a PT problem of networks, the control parameter is the number of edges added to the system per the total number of nodes. Following this convention, we introduce a variable p, which is defined as the number of cluster aggregation events per the total particle number. Whenever two clusters merge, p is increased by $\delta p = 1/N$. Since $N - 1$ aggregation events occur during all aggregation processes, the aggregation event stops at $p_f = 1 - 1/N$. p depends on t in a nonlinear way, as shown in the inset of Fig. 1(b).

In the original study of the DLCA model, the PT was not studied because the giant cluster size $G(t)$ increases monotonically as the time t increases [Fig. 1(a)]. However, we show here that when the giant cluster size G is traced as a function of p, it increases drastically, exhibiting a discontinuous PT, as shown in Fig. 1(b). This different behavior is caused by the nonlinear relationship between t and p, as shown in the inset of Fig. 1(b). When p is small, t increases almost linearly with respect to p. However, as p approaches p_f, t increases drastically in a power-law manner. As a result, G exhibits a discontinuous PT.

To check if the PT is indeed discontinuous, we use the finite-size scaling theory recently proposed for studying the

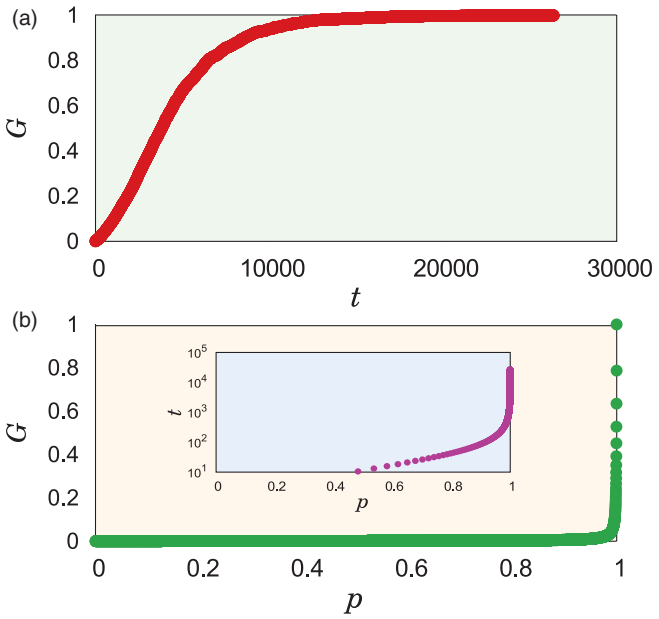

FIG. 1. (Color online) (a) Plot of the giant cluster size G vs t when particles are Brownian. The giant cluster grows continuously from $t = 0$. (b) Plot of G vs p. G grows drastically near $p_f = 1 - 1/N$. Inset: Plot of the relationship between t and p. t increases drastically but in a power-law manner as p approaches p_f. Simulations are carried out with $N = 8000$ monoparticles at $t = 0$ on 400×400 square lattices.

explosive PT [6]. For the first, we measure $G_N(p)$ for different N under the condition that the particle density ρ remains fixed. The results are shown in Figs. 2(a) and 2(b). For a given N, we pick up a $p_c(N)$ at which the increasing rate dG_N/dp is maximum. Then, the p intercept of the tangent of $G_N(p)$ at p_c, denoted by p_d, is determined as

$$p_d = p_c - \left(\left. \frac{dG_N(p)}{dp} \right|_{p_c} \right)^{-1} G_N(p_c). \tag{1}$$

Then, p_d also depends on N. We find that $dG_N(p)/dp$ at p_c increases in a power-law manner as $\sim N^{0.86}$ [Fig. 2(c)], indicating that the giant cluster size increases more drastically as N increases. *Thus, the transition is indeed discontinuous.* Near $p_d(N)$, p is rescaled as $\overline{p} = (p - p_d) dG_N(p_c)/dp$, which is then N independent. The giant cluster is then plotted as a function of $\overline{p}$. Indeed, we can see that the curves of the giant cluster sizes for different N collapse well onto a single curve [Fig. 2(d)]. Thus, the order parameter of the PT is written in the scaling form

$$G(p) \propto N^{-\beta/\bar{\nu}} f_0((p - p_d)N^{1/\bar{\nu}}), \tag{2}$$

where $f_0(x)$ is a scaling function, and $\beta = 0$ and $1/\bar{\nu} \approx 0.86 \pm 0.02$. We remark that this finite-size scaling form differs from the conventional one used in the continuous transition in the sense that p_d depends on the particle number N, which does, in turn, depend on the system size L. Whereas, in the conventional scaling form used for a continuous PT, p_d is replaced by $p_c(\infty)$, i.e., the critical point in the thermodynamic limit, which is independent of N. For comparison, the modified ER models [12–14] which were claimed to exhibit continuous PTs show $\beta/\bar{\nu} > 0$, even though their values are extremely small.

We examine the behavior of the susceptibility. The susceptibility is defined in two ways. The first is the mean cluster size $\chi_1(p) \equiv \sum_s' s^2 n_s(p) / \sum_s' s n_s(p)$, which exhibits a peak at p_{c1}. This quantity approaches p_f (defined earlier) as N increases. The susceptibility at p_{c1} increases with N as $\chi_1[p_{c1}(N)] \sim N^{0.95 \pm 0.01}$. Thus, $\chi_1(p)$ is written in the scaling form $\chi_1(p) \sim N^{\gamma_1/\bar{\nu}} f_1((p - p_d)N^{1/\bar{\nu}})$, where $f_1(x)$ is another scaling function and $\gamma_1/\bar{\nu} \approx 0.95 \pm 0.01$. The scaling behavior is confirmed numerically in Fig. 2(e). The other susceptibility is the fluctuation of the giant component sizes, i.e., $\chi_2(p) \equiv N\sqrt{\langle G_N^2(p)\rangle - \langle G_N(p)\rangle^2}$. This quantity exhibits a peak at p_{c2}. We find that $\chi_2[p_{c2}(N)] \sim N$. Thus, $\gamma_2/\bar{\nu} = 1$ and $\chi_2(p) \sim N f_2((p - p_d)N^{1/\bar{\nu}})$ with a scaling function f_2. The scaling behaviors are also confirmed numerically in Fig. 2(f).

The cluster aggregation process may be described via an asymmetric Smoluchowski equation

$$\frac{dn_s}{dp} = \sum_{i+j=s} \frac{k_i k_j'}{C(p)C'(p)} n_i n_j - \frac{n_s k_s}{C(p)} - \frac{n_s k_s'}{C'(p)}, \tag{3}$$

where $n_s \equiv N_s/N$ is the concentration of s-sized clusters, which depends on p, and $k_i k_j'/(CC')$ is a collision kernel, where $C(p) \equiv \sum_i k_i n_i$ and $C'(p) \equiv \sum_i k_i' n_i$. k_i/C and k_j'/C' are the probabilities for i- and j-sized clusters to merge, in which the prime denotes mobile clusters and the other denotes immobile clusters in simulations. Their kernels are different below.

We measure the size-dependent behaviors of k_s/C and k_s'/C' numerically. Even though it is not manifest that k_s/C and k_s'/C' follows a power law for the Brownian particle case [see Fig. 4(a)], we roughly estimate that $k_i/C \sim i^{0.3}$ and $k_j'/C' \sim j^{-0.2}$. The relation between these two exponents is mentioned later. With these exponent values, we solve the asymmetric Smoluchowski equation numerically and obtain that $\beta = 0$, $1/\bar{\nu} = 1$, $\gamma_1/\bar{\nu} = 1$, and $\gamma_2/\bar{\nu} = 1$. These obtained numerical values indicate more clearly that the transition is indeed discontinuous.

We now consider a more general case in which the velocity is given as $v_s \propto s^\eta$ [20], where s is the cluster size. To implement this case, a cluster is picked up with a probability proportional to s^η. The other rules in the numerical simulations remain the same. When clusters merge, the variable p is advanced by $1/N$, regardless of the cluster size s. The time is given by $\delta t = 1/(\sum_s N_s s^\eta)$. Intuitively, when η is small or negative, fewer large-sized clusters are selected, so their growth is suppressed. Medium-sized clusters are abundant even close to p_f, and they merge suddenly. In this case, a discontinuous PT takes place. In contrast, when η is positively large, more large-sized clusters are selected and they have more chance of colliding with other clusters, and merging into a bigger cluster. Thus, they can grow faster than smaller clusters can, so the giant cluster grows continuously and the PT is continuous. Thus we expect that there is a tricritical point η_c across which the transition type is changed. We show snapshots of the system for different

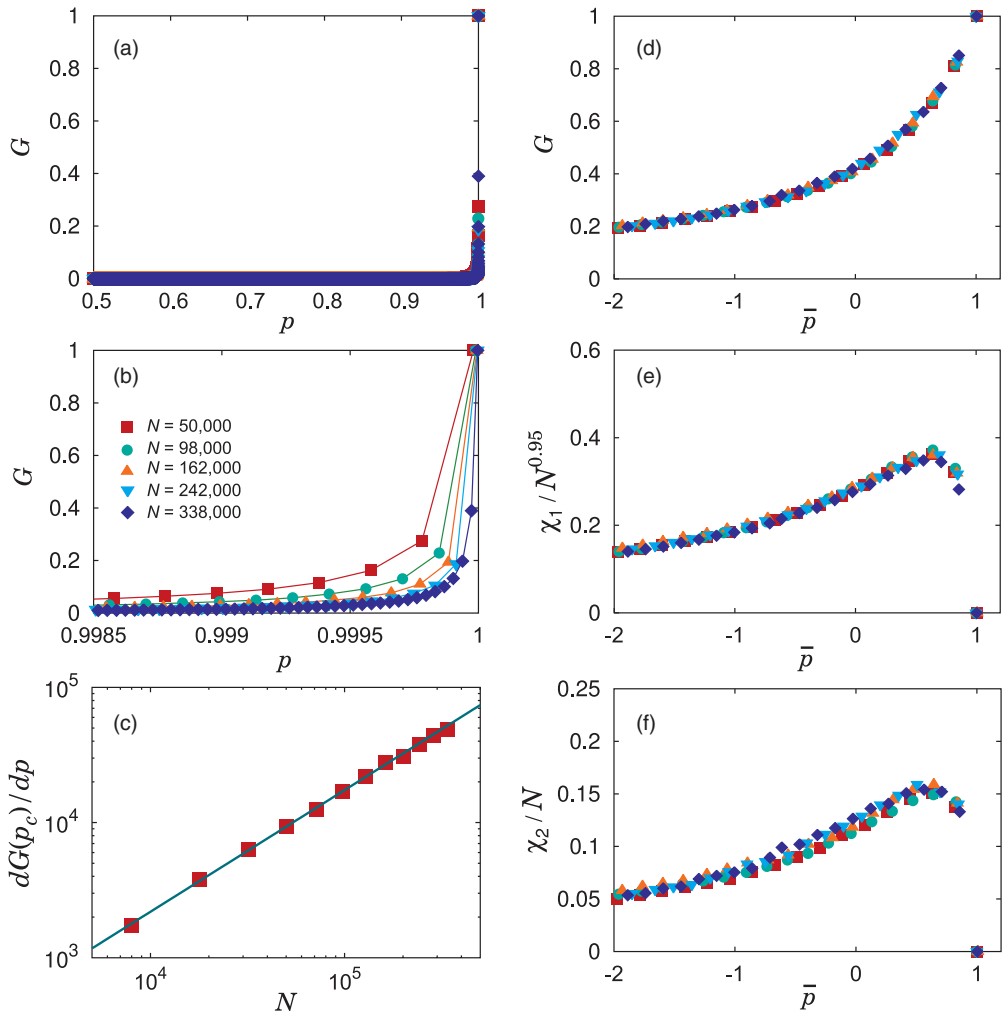

FIG. 2. (Color online) (a) Plot of G_N vs p for different particle numbers, $N = 50\,000$ (□), $N = 98\,000$ (○), $N = 162\,000$ (△), $N = 242\,000$ (▽), and $N = 338\,000$ (◇) at a fixed density $\rho = 0.05$. G_N begins to increase drastically near $p \approx 1$ and thus the data are not distinguishable for different sizes in a region that is far smaller than $p = 1$. (b) Zoomed-in plot of G_N vs p near p_c. As the system size grows, the giant cluster grows more drastically. (c) Plot of $dG_N(p)/dp$ calculated at $p_c(N)$ vs N. The slope $dG_N(p_c)/dp$ increases as $N^{0.86\pm0.02}$, indicating that it diverges in the thermodynamic limit. (d) Plot of G vs $\overline{p} \equiv (p - p_d)dG_N(p_c)/dp$ for different N. $p_d(N)$ is the p intercept of the tangent of the curve $G_N(p)$ at p_c. (e) Plot of $\chi_1/N^{0.95}$ vs $\overline{p}$. (f) Plot of χ_2/N vs $\overline{p}$. For (d), (e), and (f), the data collapse well onto a single curve.

values of η at $p = 0.99$ in Fig. 3, which support the above argument.

It has been roughly argued that the collision kernel in the Smoluchowski equation may be related to the perimeter of a cluster as $k_i \sim i^{1-1/d_f}$ [24]. However, when the selection probability is taken into consideration, the collision kernel of mobile clusters may be modified as $k_i' \sim i^{\eta+1-1/d_f}$. For the Brownian case with $\eta = -0.5$, by using the fractal dimension $d_f = 1.4$–1.5, the measured values $k_i' \sim i^{-0.2}$ for mobile clusters and $k_i \sim i^{0.3}$ for immobile clusters [Figs. 4(a) and 4(b)] are reasonable. When η is sufficiently large, such as $\eta > 0.8$, the largest cluster grows by merging small-sized clusters. In such a merging process, small-sized clusters can penetrate into the interior of the giant cluster, and then the merging probability can be independent of cluster size [Fig. 4(b)]. Thus, $k_i' \sim i^{\eta}$ and $k_i \sim$ const.

We integrate the Smoluchowski equation by using $k_i'/C' \sim i^{\eta}$ and $k_i/C \sim 1$. We find that the transition behavior changes across $\eta_c \approx 1.3$–1.4. When $\eta < \eta_c$ ($\eta > \eta_c$), as the system size increases, the percolation threshold increases to one (decreases to a finite percolation threshold). Those behaviors can be observed in Figs. 5(a) and 5(b). Moreover, for the latter case, the transition turns out to be continuous. Therefore, we conclude that there exists a tricritical point which locates at η_c. A similar behavior is observed for the DLCA model [Figs. 5(c) and 5(d)]. We also check the cluster size distribution at the percolation threshold. Indeed, the distribution obeys a power law $n_s \sim s^{-\tau}$ with $\tau = 2$ at $\eta \approx 1.4$. The exponent $\tau = 2$ is marginal between the continuous and the discontinuous PT, which was proven analytically in the cluster aggregation model [7]. Therefore, our numerical result confirm that the tricritical point locates near $\eta_c \approx 1.3$–1.4 [25,26].

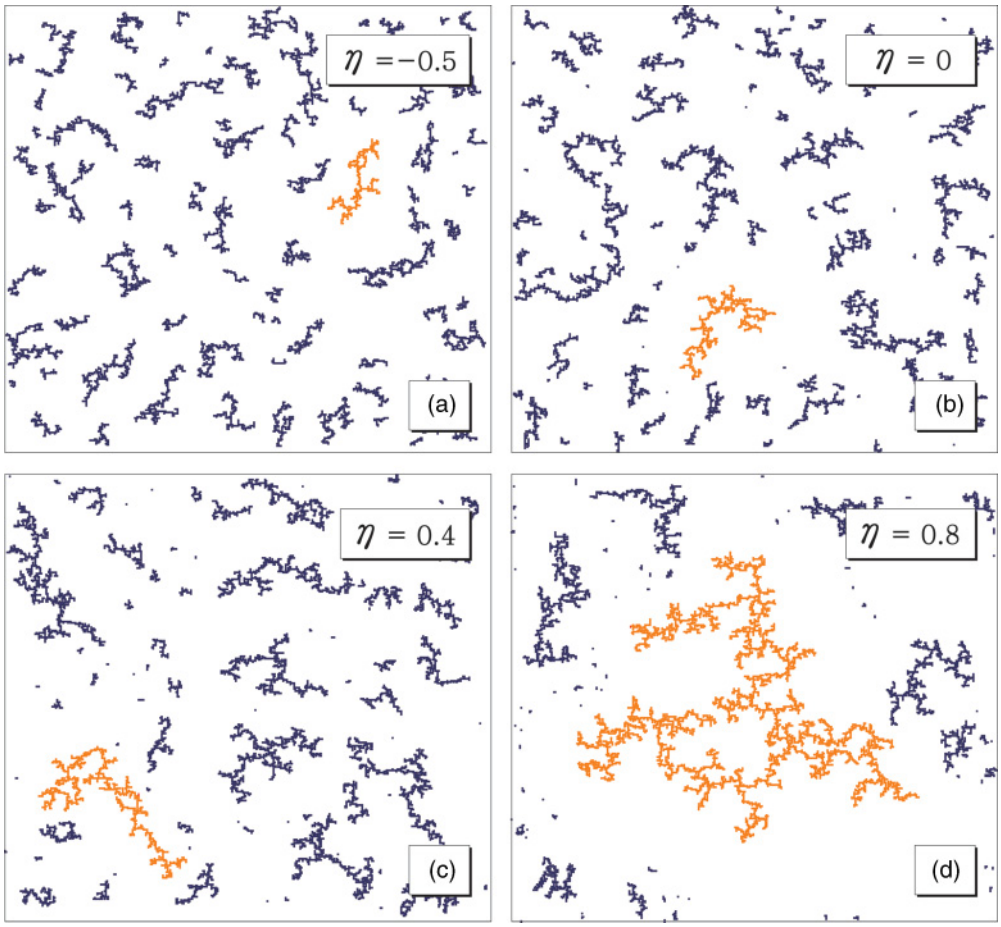

FIG. 3. (Color online) Snapshots of the system for various values of η at $p = 0.99$. The velocity of each cluster is given as $v_s \propto s^{\eta}$, where s is the cluster size. Numerical simulations are carried out for $N = 8000$ particles on $L \times L = 400 \times 400$ square lattices. Since p is fixed, the number of clusters for each case is equal. The giant cluster is represented in a different color (gray/orange). The cluster-size distribution becomes more heterogeneous as η increases.

In summary, we have studied the DLCA model as an example of real-world systems exhibiting discontinuous PT. The velocity of an s-sized cluster is given in a general form $v_s \sim s^{\eta}$. When $\eta < (>)\eta_c$, the PT is discontinuous (continuous), where a tricritical point η_c is roughly estimated to be 1.3–1.4. Since the case $\eta = -0.5$ corresponds to the Brownian particle motion in real-world systems, we can say that a discontinuous PT can take place in real-world nonequilibrium systems. We also introduced and studied an asymmetric Smoluchowski equation, and determined the tricritical point from the fact that the cluster size distribution follows a power-law behavior with exponent -2 at the tricritical point. We finally remark

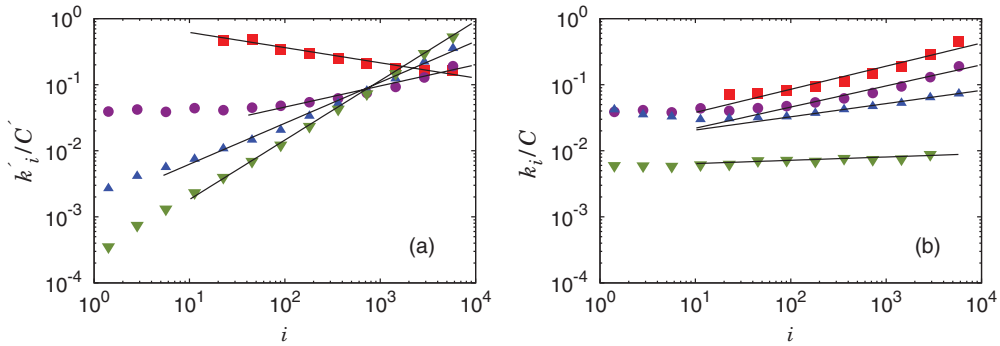

FIG. 4. (Color online) (a) Numerical estimations of k_i'/C' at p_d for $\eta = -0.5$ (□), $\eta = 0$ (○), $\eta = 0.4$ (△), and $\eta = 0.8$ (▽). Simulations are carried out for $N = 8000$ and $L = 400$. Slopes of the guidelines are -0.23 ± 0.02 for ($\eta = -0.5$), 0.32 ± 0.04 ($\eta = 0$), 0.62 ± 0.01 ($\eta = 0.4$), and 0.88 ± 0.01 ($\eta = 0.8$). (b) Numerical estimations of the k_i/C at p_d. The same symbols are used as in (a). The system size is $N = 8000$ and $L = 400$. Slopes of the guidelines are 0.35 ± 0.04 ($\eta = -0.5$), 0.32 ± 0.04 ($\eta = 0$), 0.2 ± 0.01 ($\eta = 0.4$), and 0.05 ± 0.005 ($\eta = 0.8$).

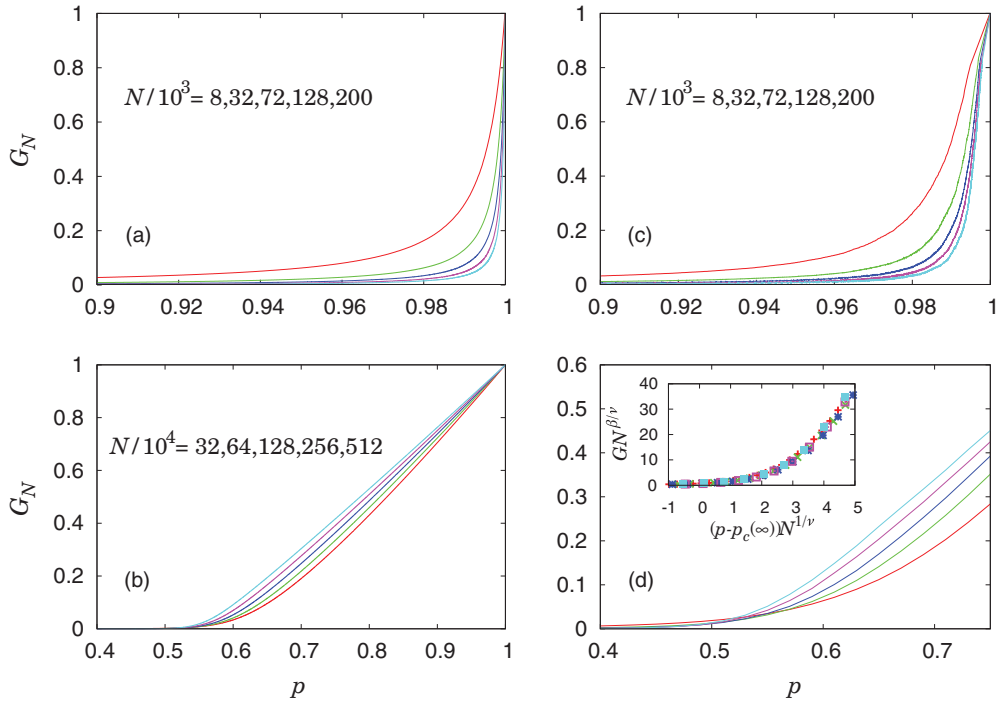

FIG. 5. (Color online) Plot of G_N vs p for the Smoluchowski equation with $k_i \sim 1$ and $k'_j \sim j^{0.8}$ (a), and $k_i \sim 1$ and $k'_j \sim j^{1.5}$ (b). As the system size grows, G_N grows more drastically and $p_c(N)$ approaches one in (a), but it decreases to $p_c(\infty) > 0$ in (b). For (b), the transition is continuous. A similar plot for the DLCA with $\eta = 0.8$ (c) and $\eta = 1.5$ (d). Similar behaviors are shown. Simulations are performed for $N/10^3 = 8$, 32, 72, 128, and 200. Inset of (d): Finite-size scaling of $G_N(p)$ for different system sizes with $1/\nu = 0.28$, $\beta/\nu = 0.5$, and $p_c(\infty) = 0.42$. These numerical values depend on η. Thus, for $\eta > \eta_c$, the critical points for different η form a critical line.

that the discovery of the explosive PT in the DLCA model was made by tracing the giant cluster size as a function of p instead of t, indicating that a discontinuous PT may be explored as a function of an unconventional parameter.

We thank D. Kim for helpful discussion. This study was supported by NRF Grants funded by the MEST (Grant No. 2010-0015066) and the NAP of KRCF (B.K.), and the Seoul Science Foundation and the Global Frontier program (Y.S.C.).

[1] S. Broadbent and J. Hammersley, Proc. Cambridge Philos. Soc. **53**, 629 (1957).
[2] D. Stauffer and A. Aharony, *Introduction to Percolation Theory* (Taylor & Francis, London, 1994).
[3] D. Achlioptas, R. M. D'Souza, and J. Spencer, Science **323**, 1453 (2009).
[4] P. Erdős and A. Rényi, Publ. Math. Inst. Hung. Acad. Sci. **5**, 17 (1960).
[5] E. J. Friedman and A. S. Landsberg, Phys. Rev. Lett. **103**, 255701 (2009).
[6] Y. S. Cho, S.-W. Kim, J. D. Noh, B. Kahng, and D. Kim, Phys. Rev. E **82**, 042102 (2010).
[7] Y. S. Cho, B. Kahng, and D. Kim, Phys. Rev. E **81**, 030103(R) (2010).
[8] A. A. Moreira, E. A. Oliveira, S. D. S. Reis, H. J. Herrmann, and J. S. Andrade Jr., Phys. Rev. E **81**, 040101(R) (2010).
[9] S. S. Manna and A. Chatterjee, Physica A **390**, 177 (2011).
[10] R. M. D'Souza and M. Mitzenmacher, Phys. Rev. Lett. **104**, 195702 (2010).
[11] N. A. M. Araújo and H. J. Herrmann, Phys. Rev. Lett. **105**, 035701 (2010).
[12] R. A. da Costa, S. N. Dorogovtsev, A. V. Goltsev, and J. F. F. Mendes, Phys. Rev. Lett. **105**, 255701 (2010).
[13] H. K. Lee, B. J. Kim, and H. Park, Phys. Rev. E **84**, 020101(R) (2011).
[14] O. Riordan and L. Warnke, Science **333**, 322 (2011)
[15] T. A. Witten Jr. and L. M. Sander, Phys. Rev. Lett. **47**, 1400 (1981).
[16] P. Meakin, Phys. Rev. Lett. **51**, 1119 (1983).
[17] M. Kolb, R. Botet, and R. Jullien, Phys. Rev. Lett. **51**, 1123 (1983).
[18] T. Vicsek and F. Family, Phys. Rev. Lett. **52**, 1669 (1984).
[19] R. Jullien, M. Kolb, and R. Botet, J. Phys. (Paris), Lett. **45**, L211 (1984).
[20] P. Meakin, T. Vicsek, and F. Family, Phys. Rev. B **31**, 564 (1985).
[21] H. G. E. Hentschel and J. M. Deutch, Phys. Rev. A **29**, 1609 (1984).
[22] A. J. Hurd and D. W. Schaefer, Phys. Rev. Lett. **54**, 1043 (1985).
[23] F. Reif, *Fundamentals of Statistical and Thermal Physics* (McGraw-Hill, New York, 1965).
[24] M. H. Ernst, E. M. Hendriks, and F. Leyvraz, J. Phys. A **17**, 2137 (1984).
[25] M. E. Fisher and M. C. Barbosa, Phys. Rev. B **43**, 11177 (1991).
[26] Y. S. Cho, D. Kim, and B. Kahng (unpublished).